Electronic Supplementary Material (ESI) for ChemComm.

Supporting information

The solid state structures of the high and low temperature phases of dimethylcadmium.

Felix Hanke,† Sarah Hindley,‡ Anthony C. Jones,§ Alexander Steiner*,§

†Dassault Systèmes BIOVIA, 334 Science Park, Cambridge CB4 0WN, UK.

‡SAFC Hitech, Power Road, Bromborough, Wirral, CH62 3QF, UK.

§Department of Chemistry, University of Liverpool, Liverpool, L69 7ZD, UK.

Email: a.steiner@liv.ac.uk

Contents:

1. Crystal data and structure refinement

Samples were contained in quartz capillaries (0.5 mm bore diameter), which were flame sealed. The capillaries were mounted vertically on the X-ray goniometer and cooled with a cold stream of N_2. Crystals of α-Me_2Cd were grown from the melt by gradually cooling the samples to 240 K. Single crystals of β-Me_2Cd were obtained by slow cooling to 150 K and repeated zone-melting using an infrared laser.[S1] Samples grown this way contained multiple single crystal domains. These produced reflections that were sufficiently separated to be suitably indexed and integrated. Heating the sample across the phase change temperatures yielded an increase in the number of domains accompanied by formation of polycrystalline material.

Crystal data were collected on a Bruker Apex diffractometer using MoK_α radiation (λ = 0.71073 Å). Crystal structures were refined with SHELX by full-matrix least squares against F^2 using all data.[S2]

α-Me_2Cd: C_2H_6Zn, $M_r = 142.47$, $T = 240$ K, tetragonal space group $P4_2/mnm$, $a = 7.195(7)$, $c = 4.118(4)$ Å, $V = 213.2(5)$ Å^3, $Z = 2$, $\rho = 2.22$ g cm^{-3}, $\mu(\mathrm{MoK}_\alpha) = 4.884$ mm^{-1}, $2\theta_{\mathrm{max}} = 50°$, 135 unique reflections, $R_{\mathrm{int}} = 0.0385$, $R1$ ($I > 2\sigma(I)$) = 0.026, $wR2$ (all data) = 0.070. The methyl groups is disordered across the crystallographic mirror plane parallel to (0,0,1) (Wyckoff symbol 8j). The Cd atom was refined anisotropically. The disordered C-atom is split by symmetry and was refined isotropically. The hydrogen atoms were restrained according to the conformation of the methyl group observed in the calculated structure using 'hard' DFIX commands.

β-Me_2Cd: C_2H_6Zn, $M_r = 142.47$, $T = 150$ K, monoclinic space group $P2_1/n$, $a = 7.483(11)$, $b = 7.711(11)$, $c = 7.734(11)$ Å, $\beta = 115.85(3)°$, $V = 401.6(10)$ Å^3, $Z = 4$, $\rho = 2.36$ g cm^{-3}, $\mu(\mathrm{MoK}_\alpha) = 5.186$ mm^{-1}, $2\theta_{\mathrm{max}} = 50°$, 600 unique reflections, $R_{\mathrm{int}} = 0.0494$, $R1$ ($I > 2\sigma(I)$) = 0.072, $wR2$ (all data) = 0.198. Cd and C atoms were refined anisotropically. The hydrogen atoms were restrained according to the conformation of the methyl group observed in the calculated structure using 'hard' DFIX commands. Note, that the coverage of reflection data was limited to 85 % due to the experimental setup, which only enabled ω rotation of the vertically aligned capillary.

(S1) R. Boese, H.-C. Weiss and D. Bläser, *Angew. Chem. Int. Ed.,* 1999, **38**, 988-992.

(S2) (a) G. M. Sheldrick, *Acta Crystallogr.,* 2008, **A64**, 112-122. (b) G. M. Sheldrick, *Acta Crystallogr.,* 2015, **C71**, 3-8.

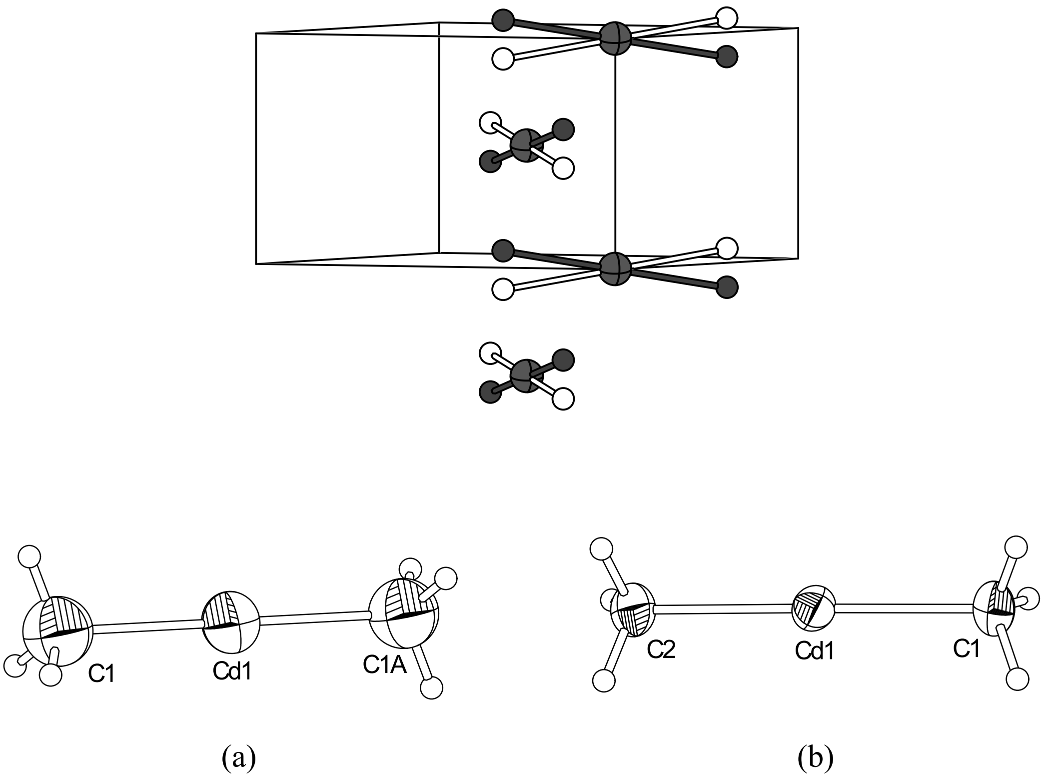

Fig. S1. Top: Disorder of carbon atom in α-Me_2Cd. Bottom: Thermal displacement ellipsoids (50% probability) for Cd and C-atoms of α-Me_2Cd (a) and β-Me_2Cd (b).

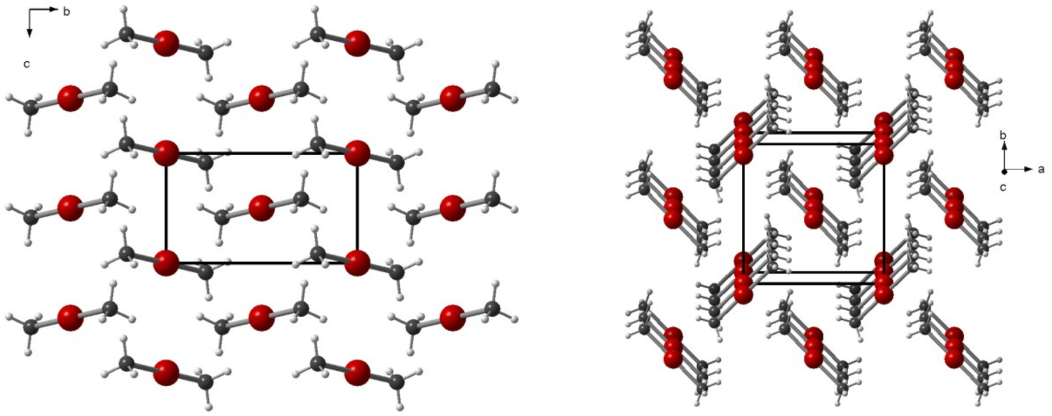

Fig. S2. Illustration of the columnar arranged structure of α-Me_2Cd (here presented as an ordered $P2_1/n$ array); columnar stacks are arranged parallel to the c-axis. The diagram on the left is viewed along the *a*-axis perpendicular to the columnar stacks; the diagram on the right is viewed along the columnar stacks.

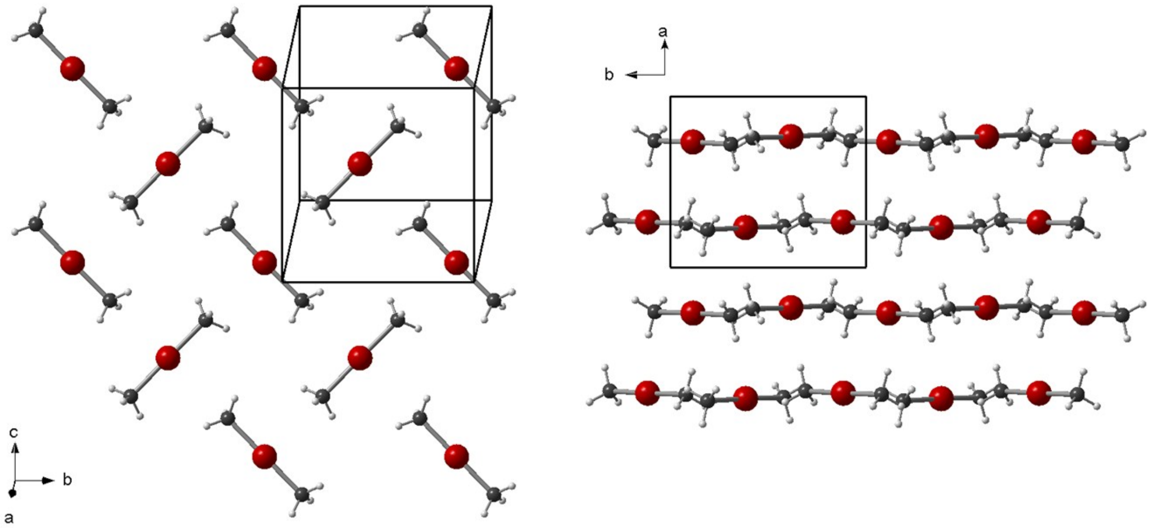

Fig. S3. Illustration of the layered structure of β-Me_2Cd; the layers are arranged parallel to (100): The diagram on the left gives a view perpendicular to the layers; the diagram on the right gives a view along the layers.

2. DFT calculations.

The DFT calculations were done with the plane wave pseudopotential code CASTEP[S3] as distributed with BIOVIA Materials Studio 2016.[S4] To optimize the unit cells, we used the PBE exchange correlation functional with the TS dispersion correction scheme.[S5] For each optimized cell, we calculated the many-body dispersion (MBD) corrected cohesive energy according to the scheme by Ambrosetti et al..[S6] The results below quote both the MBD cohesive energies and the PBE cohesive energies without dispersion corrections. From the comparison, one can see that the crystals in all cases are almost exclusively bound by dispersion forces.

Throughout this study, we used the ultrasoft pseudopotentials with the Materials Studio fine defaults for most integration settings, except for the plane wave cutoff where ultrafine settings have been applied. This corresponds to a plane wave energy cutoff of 310 eV and 350 eV for Me_2Cd and Me_2Zn respectively). The fine structure optimization thresholds are 10^{-6} eV/atom for energy changes, 0.01 eV/Å for the minimal force, and 0.02 GPa for the mininmal stress. The Brillouin zone integration was done on Monkhorst-Pack grids, chosen such that the k-point separation is no more than 0.07 1/Å.

(S3) S. J. Clark, M. D. Segall, C. J. Pickard, P. J. Hasnip, M. J. Probert, K. Refson and M. C. Payne, *Z. Krist.* 2005, **220**, 570.

(S4) Materials Studio 2016, Dassault Systèmes BIOVIA 2015.

(S5) A. Tkatchenko and M. Scheffler, *Phys. Rev. Lett.* 2009, **102**, 073005.

(S6) A. Ambrosetti, A. M. Reilly, R. A. DiStasio Jr., A. Tkatchenko, *J. Chem. Phys.* 2014, **140**, 18A508.

2.1. DFT calculations of 2x2 supercells of α-Me_2Cd and α-Me_2Zn

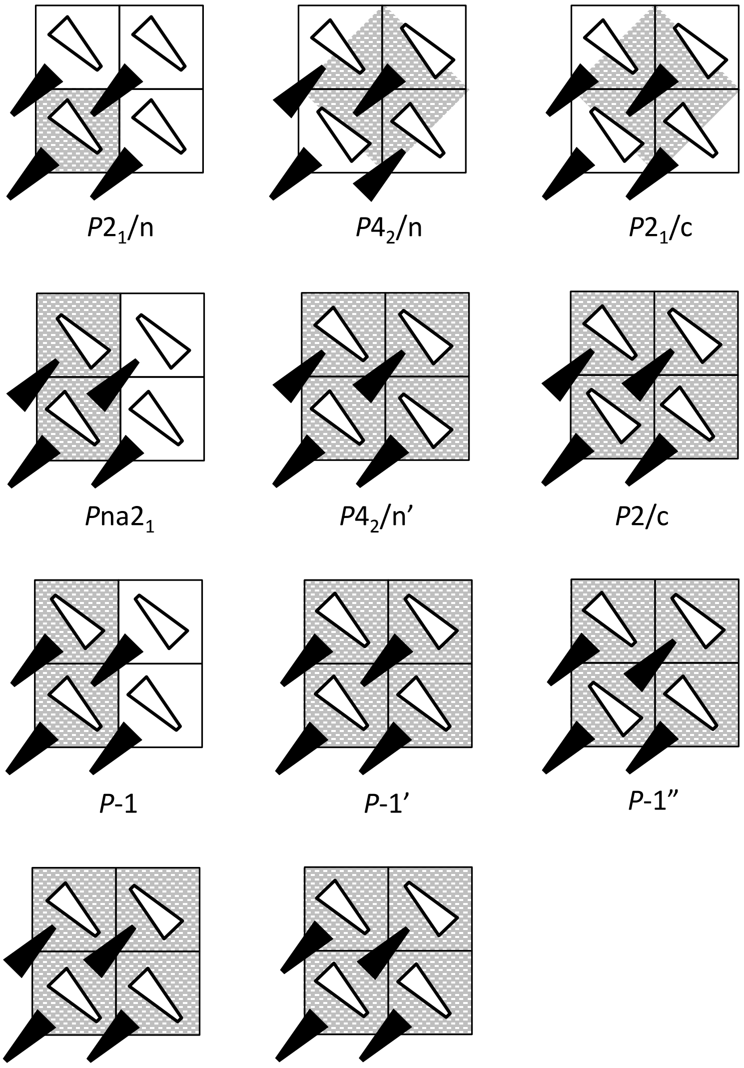

$P2_1/n$ $P4_2/n$ $P2_1/c$

$Pna2_1$ $P4_2/n'$ $P2/c$

$P\text{-}1$ $P\text{-}1'$ $P\text{-}1''$

$P1$ $P1'$

Fig. S4. Unique combinations of tilt directions for 2x2 cells of α-Me_2Cd and α-Me_2Zn. Black and white wedges indicate tilt directions for the two sets of molecules aligned parallel to (110) (metal atom at z = 0) and (1-10) (metal atom at z = ½). Grey shaded areas show the corresponding unit cells.

	unit cell [a]	Z' [b]	Sum of tilt directions [c]	number of centro-symmetric molecules [d]	number of combinations [e]
$P2_1/n$	a, a, c	0.5	4 + 4	8	4
$P4_2/n$	$\sqrt{2}$a, $\sqrt{2}$a, *c*	0.5	0 + 0	8	4
$P2_1/c$	*c*, $\sqrt{2}$a, $\sqrt{2}$a	1	4 + 0	8	8
$Pna2_1$	2a, c, a	1	0 + 0	0	8
$P4_2/n'$	2a, 2a, c	1	0 + 0	0	8
$P2/c$	2a, c, 2a	2	0 + 0	4	16
P-1	a, 2a, c	2	4 + 0	4	16
P-1'	2a, 2a, c	4	4 + 2	4	32
P-1"	2a, 2a, c	4	2 + 0	4	32
$P1$	2a, 2a, c	8	2 + 0	0	64
$P1'$	2a, 2a, c	8	2 + 2	0	64

Table S1. Unique combinations of tilt directions for 2x2 cells of $\alpha\text{-Me}_2\text{Zn}$ and $\alpha\text{-Me}_2\text{Cd}$. [a] *a* and *c* refer to parameters of 1x1 cell. [b] Z' = number of molecules per asymmetric unit. [c] Surplus of one tilt direction over the other for molecules aligned parallel to (110) and (1-10) in 2x2 cell, respectively (separated by '+' sign). [d] Number of molecules per 2x2 cell that are located on crystallographic inversion centres. [e] Number of all possible combinations for each arrangement; the total number of combinations for a 2x2 cell is $2^8 = 256$.

	α-Me_2Cd		α-Me_2Zn	
	MBD*	PBE only	MBD*	PBE only
$P2_1/n$	0.61	0.11	0.53	0.066
$P4_2/n$	0.64	0.14	0.55	0.079
$P2_1/c$	0.64	0.14	0.55	0.080
$Pna2_1$	0.60	0.11	0.52	0.066
$P4_2/n'$	0.60	0.11	0.52	0.067
$P2/c$	0.60	0.11	0.52	0.066
P-1	0.60	0.11	0.52	0.070
P-1'	0.60	0.11	0.52	0.069
P-1"	0.60	0.11	0.52	0.066
$P1$	0.60	0.11	0.52	0.067
$P1'$	0.60	0.11	0.52	0.067

Table S2. Cohesive energies (eV per molecule) for the 2x2 cells of α-Me_2Zn and α-Me_2Cd.

Me$_2$Cd	*a* (Å)	*b* (Å)	*c* (Å)	α (°)	β (°)	γ (°)	*V* (Å^3) [a]
*P*2$_1$/n	7.12	7.30	4.01	90.00	93.11	90.00	832.5
*P*4$_2$/n	10.31	10.31	3.88	90.00	90.00	90.00	824.9
*P*2$_1$/c	3.89	10.29	10.28	90.00	91.35	90.00	822.7
*P*na2$_1$	14.36	4.00	7.27	90.00	90.00	90.00	835.2
*P*4$_2$/n'	14.55	14.55	3.95	90.00	90.00	90.00	836.2
*P*2/c	14.56	3.95	14.56	90.00	90.05	90.00	837.4
P-1	7.29	14.54	3.97	88.68	91.22	89.89	841.2
P-1'	14.55	14.57	3.97	88.11	90.66	89.91	841.1
P-1"	14.56	14.56	3.96	89.29	89.29	90.05	839.4
*P*1	14.55	14.55	3.96	89.32	90.67	90.01	838.2
*P*1'	14.54	14.57	3.96	88.68	90.00	90.00	838.7

Me$_2$Zn	*a* (Å)	*b* (Å)	*c* (Å)	α (°)	β (°)	γ (°)	*V* (Å^3) [a]
*P*2$_1$/n	6.84	6.91	4.02	90.00	88.70	90.00	759.8
*P*4$_2$/n	9.72	9.72.	3.96	90.00	90.00	90.00	748.3
*P*2$_1$/c	3.97	9.72	9.72	90.00	90.47	90.00	750.1
*P*na2$_1$	13.63	4.06	6.88	90.00	90.00	90.00	761.4
*P*4$_2$/n'	13.73	13.73	4.06	90.00	90.00	90.00	765.4
*P*2/c	13.73	4.06	13.74	90.00	90.01	90.00	765.9
P-1	6.88	13.73	4.07	89.53	90.48	89.99	768.9
P-1'	13.74	13.73	4.07	89.32	90.24	90.00	767.7
P-1"	13.73	13.73	4.06	89.80	89.80	90.00	765.4
*P*1	13.72	13.73	4.06	89.78	90.22	90.01	764.8
*P*1'	13.73	13.73	4.06	89.58	90.00	90.00	765.3

Table S3. Cell parameters of unit cells of possible 2x2 cell arrangements of α-Me$_2$Cd (top) and α-Me$_2$Zn (bottom) from DFT calculations. [a] Volumes are based on 2x2 cell.

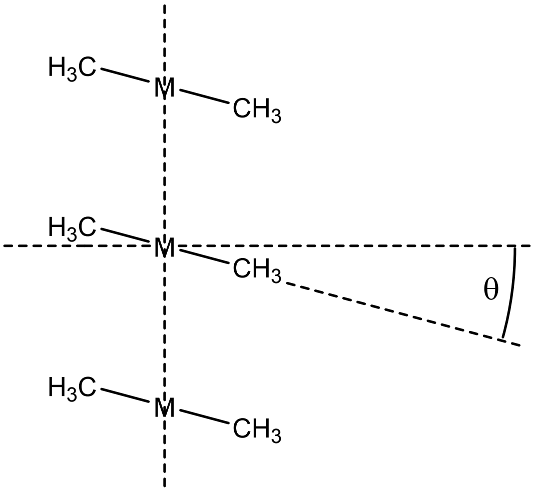

	α-Me_2Cd		α-Me_2Zn	
	θ (°)	*d*(M...M) (Å)	θ (°)	*d*(M...M) (Å)
$P2_1$/n	12.59	4.01	11.67	4.02
$P4_2$/n	6.86	3.88	7.46	3.96
$P2_1$/c	6.99 - 8.58	3.89	7.34 - 7.91	3.97
*P*na2_1	9.05	4.00	7.47	4.06
$P4_2$/n'	7.33	3.95	7.52	4.06
*P*2/c	7.21 - 7.25	3.95	7.49 - 7.50	4.06
P-1	7.37 - 9.39	3.97	7.52 - 8.18	4.07
P-1'	6.50 - 9.48	3.97	7.18 - 8.12	4.07
P-1"	6.37 - 8.63	3.96	7.35 - 7.91	4.06
*P*1	6.40 - 8.55	3.96	7.25 - 7.85	4.06
*P*1'	6.57 - 8.70	3.96	7.27 - 7.86	4.06

Table S4. Tilt angles θ of molecules of α-Me_2Cd and of α-Me_2Zn with respect to the orthogonal of M...M vector (= main axis of stack) and distance *d*(M...M) between metal atoms in a stack.

2.2. Probing the potential disorder along columnar stacks of the α-phase of Me_2Cd

Hypothetically, disorder could also occur along the stacks of molecules that run parallel to the *c*-axis. Figure S5 shows the ordered structure **A** and the theoretical disordered structure **B**, which exhibits two different, randomly distributed tilt directions (denoted + and −). In **B**, however, the methyl groups of every molecule must rotate 60º with respect to the **A**-form in order to minimise repulsion between hydrogen atoms of neighbouring molecules (relative rotations are denoted **a** for 0º and **b** for 60º).

We have applied DFT calculations in order to examine the relative stabilities of **A** and **B**. Neighbouring molecules of disordered stacks of **B** show two different kind of interactions: One between molecules of the same tilt direction (b+ and b+, as well as b– and b–) and the other between molecules of opposing tilt directions (b+ and b–). Structures based on 1x1 cells of **B**(+ +) and **B**(+ −) (see Fig. S6 and Table S5) show noticeably lower cohesive energies than **A**.

These calculations also indicate that a potential dynamic disorder featuring unhindered 'free' rotations of methyl groups is less likely as methyl groups of neighbouring molecules are interlocked. Hence, a full rotation may only be possible in a concerted mechanism by which the rotation of methyl groups and the tilting of all neighbouring molecules are suitably synchronised. This would be energetically unfavourable since large numbers of molecules would have to be displaced from their equilibrium positions simultaneously.

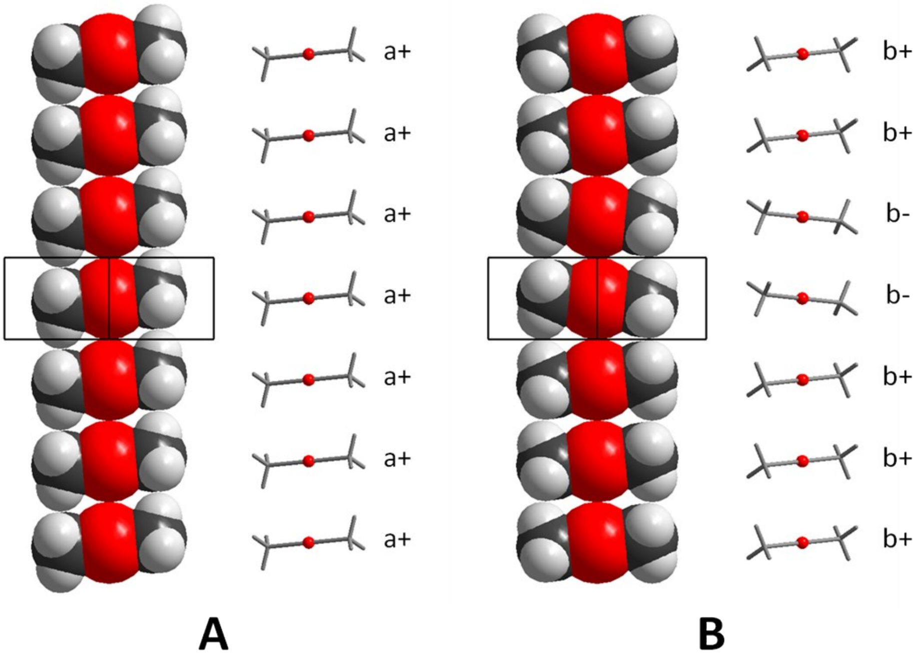

Fig. S5. Ordered structure **A** and a hypothetical disordered structure **B**. **a** and **b** denote relative rotation of methyl group (0º and 60º, respectively), while + and – represent one of the two tilt directions.

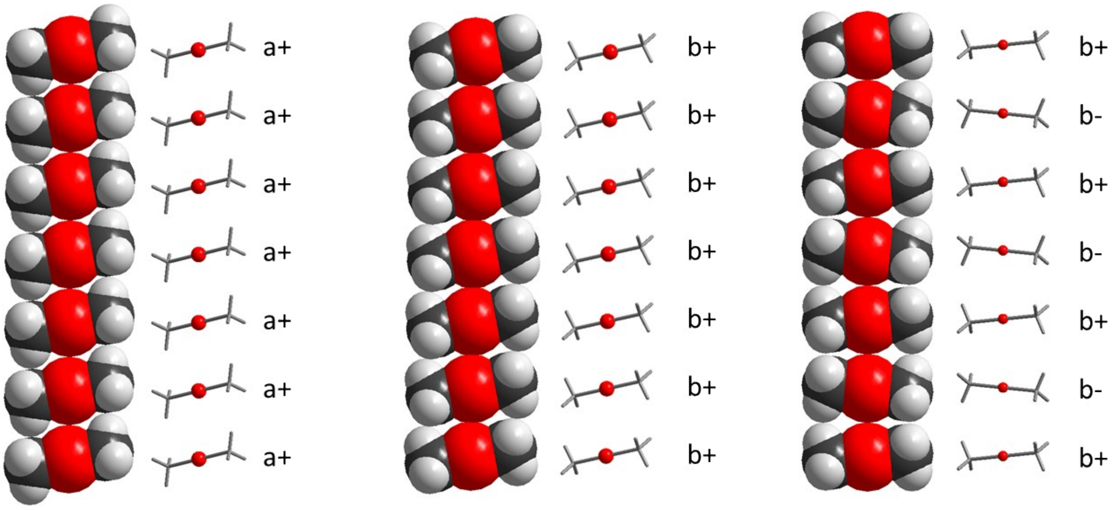

A **B**(+ +) **B**(+ −)

Fig. S6. DFT optimised structures of **A** (which corresponds to $P2_1$/n in Table S2), **B**(+ +) and **B**(+ −).

	MBD*	PBE only
A	0.61	0.11
B(+ +)	0.56	0.08
B(+ −)	0.55	0.08

Table S5. Cohesive energies (eV per molecule) for 1x1 cells.

2.3. DFT calculations of β-Me_2Cd and β-Me_2Zn.

	MBD*	PBE only
β-Me_2Cd	0.59	0.11
β-Me_2Zn	0.51	0.066

Table S6. Cohesive energies (eV per molecule) for β-Me_2Cd and β-Me_2Zn.

	a (Å)	b (Å)	c (Å)	α (°)	β (°)	γ (°)	V (Å^3)
β-Me_2Cd	7.42	7.96	7.92	90	115.1	90	423.6
β-Me_2Zn	7.33	7.63	7.60	90	114.0	90	388.3

Table S7. Unit cell parameters of β-Me_2Zn and β-Me_2Cd from DFT.

	M-C (Å)	C-M-C (°)
β-Me_2Cd	2.151, 2.153	179.0
β-Me_2Zn	1.932, 1.934	179.2

Table S8. Bond lengths and angles for β-Me_2Cd and β-Me_2Zn from DFT.

3. Assessment of the conformation of the methyl groups of β-Me_2Cd

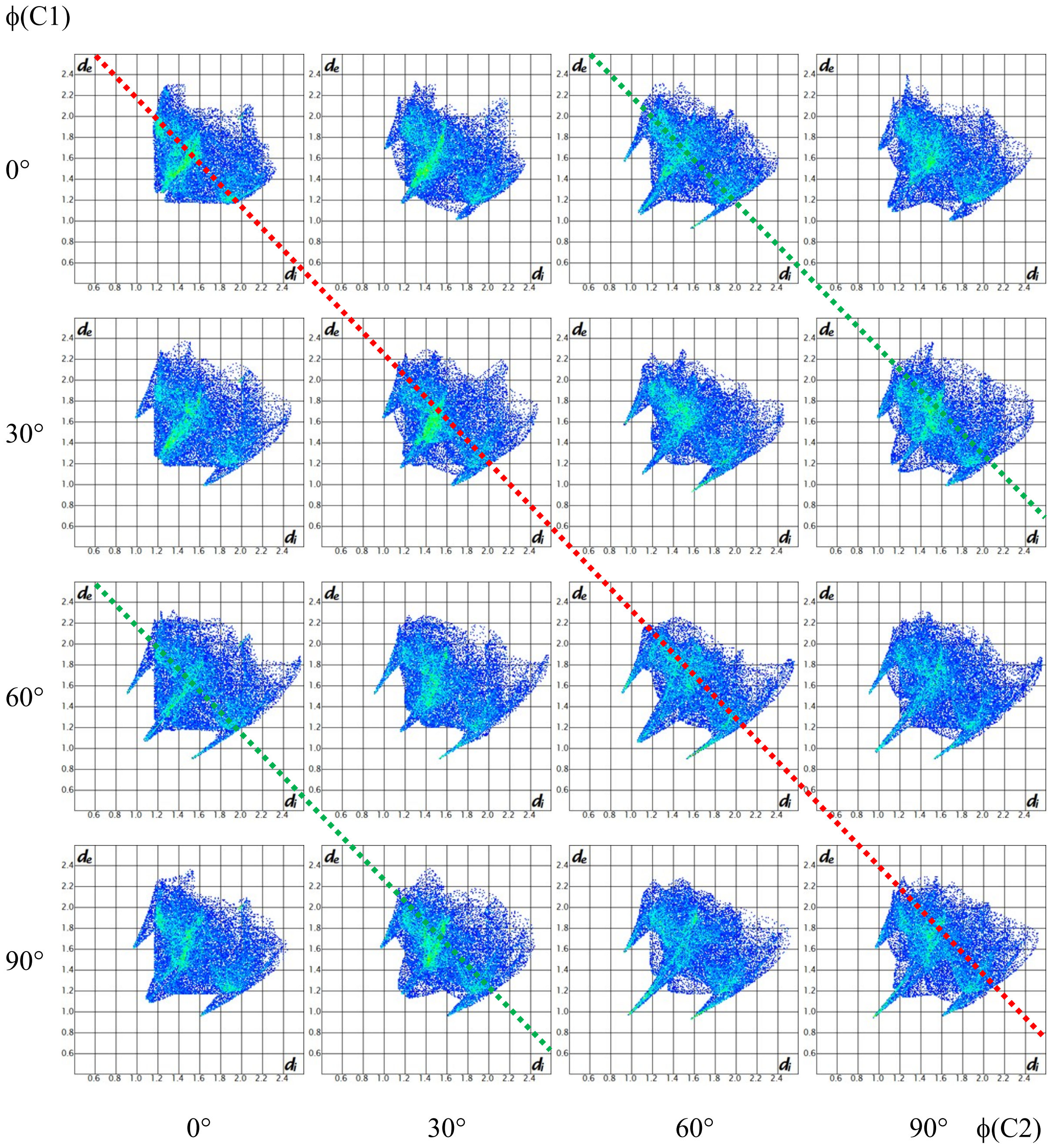

Fig. S7. Hirshfeld surface analysis[S7] was used to determine the most appropriate conformation of the methyl groups in the structure of β-Me_2Cd. Structures of various conformations ϕ(C1)/ϕ(C2) were assessed using fingerprint plots {angles ϕ(C1) and ϕ(C2) represent the rotation of methyl groups at C1 and C2 with respect to a vector orthogonal to the lattice plane (100) }. Each point in these plots corresponds to a unique d_e/d_i pair (d_e is the distance from the Hirshfeld surface to the nearest nucleus outside the surface; d_i is the distance to the nearest nucleus inside the surface). These plots are pseudo-mirrored along the $d_e = d_i$ diagonal. Spikes along the central diagonal indicate short H···H contacts, while the spikes at the wings are due to short H···Cd interactions. Eclipsed conformers are displayed along dotted red lines [$\phi(C1) = \phi(C2)$] and staggered conformers along dotted green lines [$\phi(C1) = \phi(C2) + 60°$]. It becomes clear from these plots that the conformer at $\phi(C1) = \phi(C2) = 0°$ (see structure diagram below) shows the most suitable intermolecular distances. All other conformers generate excessively short contacts that are well below the sum of Van-der-Waals radii as indicated by spikes in the fingerprint plots. Also note that these structures tend to generate fringes in the region of longer contacts, which is symptomatic of void space.

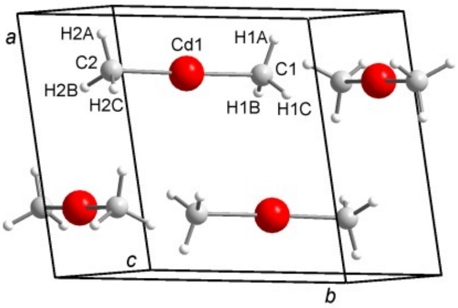

$\phi(C1) = \phi(C2) = 0°$

(S7) (a) J. J. McKinnon, D. Jayatilaka M. A. Spackman, *Chem. Commun.,* 2007, 3814. (b) M. A. Spackman, D. Jayatilaka, *CrystEngComm,* 2009, **11**, 19.